

End-To-End Optimization of Online Neural Network-supported Two-Stage Dereverberation for Hearing Devices

Jean-Marie Lemerrier*, Joachim Thiemann†, Raphael Koning†, Timo Gerkmann*

*Signal Processing (SP), Universität Hamburg, Germany

†Advanced Bionics, Hanover, Germany

{firstname.lastname}@uni-hamburg.de, {firstname.lastname}@advancedbionics.com

Abstract—A two-stage online dereverberation algorithm for hearing devices is presented in this paper. The approach combines a multi-channel multi-frame linear filtering approach with a single-channel single-frame post-filter. Both components rely on power spectral density (PSD) estimates provided by deep neural networks (DNNs). This contribution extends our prior work, which shows that directly optimizing for a criterion at the output of the multi-channel linear filtering stage results in a more efficient dereverberation, as compared to placing the criterion at the output of the DNN to optimize the PSD estimation. In the present work, we show that the dereverberation performance of the proposed first stage particularly improves the early-to-mid reverberation ratio if trained end-to-end. We thus argue that it can be combined with a post-filtering stage which benefits from the early-to-mid ratio improvement and is consequently able to efficiently suppress the residual late reverberation. This proposed two stage procedure is shown to be both very effective in terms of dereverberation performance and computational demands. Furthermore, the proposed system can be adapted to the needs of different types of hearing-device users by controlling the amount of reduction of early reflections. The proposed system outperforms the previously proposed end-to-end DNN-supported linear filtering algorithm, as well as other traditional approaches, based on an evaluation using the noise-free version of the WHAMR! dataset.

Index Terms—dereverberation, neural network, end-to-end learning, hearing devices

I. INTRODUCTION

Communication and hearing devices require modules aiming at suppressing undesired parts of the signal to improve the speech quality and intelligibility. Reverberation is one of such distortions caused by room acoustics, and is characterized by multiple reflections on the room enclosures. Late reflections particularly degrade the speech signal and may result in a reduced intelligibility [1].

Traditional approaches were proposed for dereverberation such as spectral enhancement [2], beamforming [3], a combination of both [4], coherence weighting [5], [6], and linear-prediction based approaches such as the well-known weighted-prediction error (WPE) algorithm [7], [8]. WPE computes an auto-regressive multi-channel filter in the short-time spectrum and applies it to a delayed group of reverberant speech frames. This approach is able to partially cancel late reverberation

while inherently preserving parts of the early reflections, thus improving speech intelligibility for normal and hearing-supported listeners [9].

WPE and its extensions require the prior estimation of the anechoic speech power spectrum density (PSD), which is modelled for instance through the speech periodogram [7] or a power-compressed periodogram corresponding to sparse priors [8], by an autoregressive process [10] or through non-negative matrix factorization [11]. A deep neural network (DNN) was first introduced in [12] to model the anechoic PSD, thus avoiding the use of an iterative refinement process.

Instead of providing parameters for linear prediction as in e.g. [12], [13], DNNs were also proposed to perform direct mapping in the time-frequency magnitude domain [14], complex domain [15] or in the time-domain [16].

As hearing devices are expected to operate in real-time situations, the dereverberation techniques should support low-latency online processing and adapt to changing room acoustics. Such online adaptive approaches were introduced, based on either Kalman filtering [17], [18] or on a recursive least squares (RLS) adapted WPE, which can be seen a special case of Kalman filtering [19]. Strategies for handling the case of speakers changing positions were introduced in [18], [19]. In the RLS-WPE framework, the PSD is either estimated by recursive smoothing of the reverberant signal [19] or by a DNN [20].

In the previously cited works, the DNN is trained towards PSD estimation, although this stage is only a front-end to further RLS-WPE-based dereverberation algorithms. So-called “end-to-end techniques” aim to solve this mismatch by using a criterion placed at the output of the complete algorithm to train the DNN. End-to-end techniques using an Automatic Speech Recognition (ASR) criterion were designed to refine the front-end DNN handling e.g. speech separation [21], denoising [22], or multiple tasks [23]. An end-to-end procedure using ASR was also introduced in [24] to optimize a DNN used for online dereverberation. In contrast, we proposed to use a criterion directly on the output signal rather than using ASR in our previous work [25]. We argued that it was more likely to improve instrumentally predicted speech intelligibility and quality. It also enabled us to use different target signals and

corresponding WPE parameters to make our approach adapt to the needs of different hearing-aid users categories: hearing-aid (HA) users on the one hand benefiting from early reflections like normal listeners [9], and cochlear implant (CI) users on the other hand which do not benefit from early reflections [26].

We noticed in our previous study [25] that although the energy residing in the moderate reverberation range corresponding to the filter length was particularly suppressed when training the approach in an end-to-end fashion, residual late reverberation could still be heard at the output. A further processing stage could be dedicated to removing this residual reverberation, as increasing the length of the linear filters results in rapidly increasing computational complexity and training difficulty. Hybrid approaches using of such cascaded DNN-assisted stages have been proposed for dereverberation [27] or joint dereverberation, separation and denoising [13], [23], [28].

The contributions of the present work are thus threefold: first, we introduce metrics to measure the energies in various reverberation ranges in order to investigate the differences between the previously cited WPE-based approaches and our approach. Second, we propose to use a second DNN-supported stage based on single-frame non-linear magnitude filtering, and show that it significantly suppresses the residual late reverberation at the output of WPE. We show with the newly introduced metrics that this latter stage particularly benefits from strong dereverberation within the linear filter range obtained with the previous end-to-end WPE approach. Finally, we customize the presented two-stage algorithm to hearing listener classes by adapting the training target and algorithm parameters as in previous work [25].

The rest of this paper is organized as follows. In Section II, the online DNN-WPE dereverberation scheme is summarized. Section III presents the DNN-supported post-filter and describes the used end-to-end training procedure. In Section IV, we describe the experimental setup and introduce metrics in order to detail the dereverberation performance in various reverberation ranges. The results are presented and discussed in Section V.

II. SIGNAL MODEL AND DNN-SUPPORTED WPE DEREVERBERATION

A. Signal model

In the short-time Fourier transform (STFT) domain using the subband-filtering approximation [7], the reverberant speech $\mathbf{x} \in \mathbb{C}^D$ is obtained at the D -microphone array by convolution of the anechoic speech s and the room impulse responses (RIRs) $\mathbf{H} \in \mathbb{C}^{D \times D}$ with length N :

$$\mathbf{x}_{t,f} = \sum_{\tau=0}^N \mathbf{H}_{\tau,f} s_{t-\tau,f} = \mathbf{d}_{t,f} + \mathbf{e}_{t,f} + \mathbf{r}_{t,f} + \mathbf{u}_{t,f}, \quad (1)$$

where t denotes the time frame index and f the frequency bin, which we will drop when not needed. \mathbf{d} denotes the direct path, \mathbf{e} the early reflections component, \mathbf{r} the late reverberation and \mathbf{u} an error term comprising modelling errors and background noise. The early reflections component \mathbf{e} was shown to contribute to speech quality and intelligibility for

normal and HA listeners [9] but not for CI users, particularly in highly-reverberant scenarios [26]. Therefore, we propose that the dereverberation objective is to retrieve $\boldsymbol{\nu} = \mathbf{d} + \mathbf{e}$ for HA listeners and $\boldsymbol{\nu} = \mathbf{d}$ for CI listeners.

B. WPE dereverberation

In relation to the subband reverberant model in (1), the WPE algorithm [7] uses an auto-regressive model to approximate the late reverberation \mathbf{r} . Based on a zero-mean time-varying Gaussian model on the STFT anechoic speech s with time-frequency dependent PSD $\lambda_{t,f}$, a multi-channel filter $\mathbf{G} \in \mathbb{C}^{DK \times D}$ with K taps is estimated. This filter aims at representing the inverse of the late tail of the RIRs \mathbf{H} , such that the target $\boldsymbol{\nu}$ can be obtained through linear prediction, with a delay Δ avoiding undesired short-time speech cancellations, which also leads to preserving parts of the early reflections. By disregarding the error term \mathbf{u} in (1) in noiseless scenarios, we obtain:

$$\boldsymbol{\nu}_{t,f}^{(\text{WPE})} = \mathbf{x}_{t,f} - \mathbf{G}_{t,f}^H \mathbf{X}_{t-\Delta,f}, \quad (2)$$

where $\mathbf{X}_{t-\Delta,f} = [\mathbf{x}_{t-\Delta,f}^T, \dots, \mathbf{x}_{t-\Delta-K+1,f}^T]^T \in \mathbb{C}^{DK}$.

In order to obtain an adaptive and real-time capable approach, RLS-WPE was proposed in [19], where the WPE filter \mathbf{G} is recursively updated along time. RLS-WPE can be seen as a special case of Kalman filtering, in which the target covariance matrix is replaced by the scaled identity matrix $\lambda^{(\text{WPE})} \mathbf{I}$, and the weight state error matrix is simply updated by dividing by the recursive factor $\alpha^{(\text{WPE})}$ instead of following the usual Markov model [18]:

$$\mathbf{K}_{t,f} = \frac{(1 - \alpha^{(\text{WPE})}) \mathbf{R}_{t-1,f}^{-1} \mathbf{X}_{t-\Delta,f}}{\alpha^{(\text{WPE})} \lambda_{t,f}^{(\text{WPE})} + (1 - \alpha^{(\text{WPE})}) \mathbf{X}_{t-\Delta,f}^H \mathbf{R}_{t-1,f}^{-1} \mathbf{X}_{t-\Delta,f}}, \quad (3)$$

$$\mathbf{R}_{t,f}^{-1} = \frac{1}{\alpha^{(\text{WPE})}} \mathbf{R}_{t-1,f}^{-1} - \frac{1}{\alpha^{(\text{WPE})}} \mathbf{K}_{t,f} \mathbf{X}_{t-\Delta,f}^T \mathbf{R}_{t-1,f}^{-1}, \quad (4)$$

$$\mathbf{G}_{t,f} = \mathbf{G}_{t-1,f} + \mathbf{K}_{t,f} (\mathbf{x}_{t,f} - \mathbf{G}_{t-1,f}^H \mathbf{X}_{t-\Delta,f})^H. \quad (5)$$

$\mathbf{K} \in \mathbb{C}^{DK}$ is the Kalman gain, $\mathbf{R} \in \mathbb{C}^{DK \times DK}$ the covariance of the delayed reverberant signal buffer $\mathbf{X}_{t-\Delta,f}$ weighted by the PSD estimate $\lambda_{t,f}^{(\text{WPE})}$, and $\alpha^{(\text{WPE})}$ the forgetting factor.

In non-idealistic scenarios, the term \mathbf{u} is not zero. Therefore, a regularization parameter $\epsilon > 0$ is added to the denominator of (3) which can be seen as a form of spectral flooring as used in traditional spectral enhancement schemes [4], [6], [29]. Although it is not *per se* a denoising solution and we still consider scenarios where noise is negligible in comparison to reverberation, adding this parameter helps increasing the robustness of WPE to noise, numerical instabilities and modelling errors. On the other hand, setting ϵ to a high value will excessively attenuate the relative variations of the Kalman denominator, which mitigates the benefits of variance-normalization as explained in [30]. A value of $\epsilon^* = 0.001$ was picked based on the performance of the WPE algorithm using oracle target PSD.

C. DNN-based PSD estimation

The anechoic speech PSD estimate $\lambda_{t,f}^{(\text{WPE})}$ is obtained at each time step t , either by recursive smoothing of the reverberant periodogram [19] or with help of a DNN [20]. A block diagram of the DNN-WPE algorithm as proposed in [20] is given in Fig. 1, as the first stage up to $\nu^{(\text{WPE})}$. In this approach, the channel-averaged magnitude frame $|\bar{x}_t|$ is fed as input to a recurrent neural network $\text{MaskNet}_{\text{WPE}}$ with hidden state h_{WPE} and the output being a real-valued mask $\mathcal{M}_{t,f}^{(\text{WPE})}$. The PSD estimate is then obtained by time-frequency masking:

$$\lambda_{t,f}^{(\text{WPE})} = (\mathcal{M}_{t,f}^{(\text{WPE})} \odot |\bar{x}_{t,f}|)^2, \quad (6)$$

where \odot represents the Hadamard element-wise product.

In [12], [20], the DNN is optimized with a mean-squared error (MSE) criterion on the masked output. In contrast, in our previous work [25] we proposed to use the Kullback-Leibler (KL) divergence [31]:

$$\mathcal{L}_{\text{DNN-WPE}} = \text{KL}(\mathcal{M}_{t,f}^{(\text{WPE})} \odot |\bar{x}_{t,f}|, |\nu_{t,f}|), \quad (7)$$

with:

$$\text{KL}(\mathbf{X}, \mathbf{Y}) = \mathbb{E}_{t,f} \left[\mathbf{X}_{t,f} \log \frac{\mathbf{X}_{t,f}}{\mathbf{Y}_{t,f}} + |\mathbf{X}_{t,f} - \mathbf{Y}_{t,f}| \right]. \quad (8)$$

This loss function indeed led to better results in our experiments. This can be explained by the fact that (8) puts more weight on low-energy bins in comparison to the MSE loss, which is a good fit for dereverberation.

D. End-to-End Training Procedure

1) *End-to-end criterion and objectives:* In [25], we showed that the mismatch between the DNN-optimization criterion (7) and the dereverberation task limited the overall performance. On the other hand, we argued that using ASR as an end-to-end training criterion, as is done in [24], is not necessarily the best choice in order to optimize a dereverberation algorithm for hearing-aid users. The first reason is that the resulting scheme could not be adapted to specific user categories, although these benefit from different speech cues. Namely, HA listeners are shown to benefit from early reflections [9] where CI listeners do not significantly benefit from those, in particular in highly reverberant scenarios where early reflections degrade intelligibility [26]. The second reason is that by nature, the dereverberation scheme will provide the best representation possible for ASR, which may be not the optimal representation in terms of quality and intelligibility for a human listener.

We therefore proposed an end-to-end training procedure where the optimization criterion is placed in the time-frequency domain at the output of the DNN-WPE algorithm, thus including the back-end WPE into DNN optimization:

$$\mathcal{L}_{\text{E2E-WPE}} = \text{KL}(|\nu_{t,f}^{(\text{WPE})}|, |\nu_{t,f}|). \quad (9)$$

2) *Initialization period:* An important practical aspect of this study focuses on handling the initialization period of the RLS-WPE algorithm. During this interval of L_i time frames, the filter \mathbf{G} has not yet converged to a stable value, reducing dereverberation performance.

Therefore, rather than relying on a hypothetical shortening of this period through implicit PSD optimization [24], we choose to exclude this initialization period from training.

3) *Training strategies:* We showed in [25] that the best performance was obtained with the so-called **E2Ep-WPE** approach, where the network $\text{MaskNet}_{\text{WPE}}$ is first pre-trained with (7) and fine-tuned with (9) using the proposed end-to-end procedure. The end-to-end training procedure is presented in [25] and an extension to the two-stage dereverberation scheme is given in Algorithm 1 in the next section.

III. RESIDUAL REVERBERATION SUPPRESSION

A. Signal model

As shown in Section V below, training DNN-WPE in an end-to-end fashion helps suppressing most of the reverberant signal immediately following the target range, that is, up to L_m , which we refer to as the *moderate reverberation* range.

We therefore refine the reverberant signal model (1) as:

$$\mathbf{x}_{t,f} = \sum_{\tau=0}^N \mathbf{H}_{\tau,f} s_{t-\tau,f} = \nu_{t,f} + \mathbf{m}_{t,f} + \phi_{t,f} + \mathbf{u}_{t,f}, \quad (10)$$

where the undesired reverberant signal in (1) (corresponding to \mathbf{r} and $\mathbf{e} + \mathbf{r}$ in the HA and CI case respectively) is split in the *moderate* reverberant signal \mathbf{m} and the *final* reverberant signal ϕ , defined as:

$$\mathbf{m}_{t,f} = \sum_{\tau=\Delta}^{\Delta+L_m-1} \mathbf{H}_{\tau,f} s_{t-\tau,f}, \quad (11)$$

$$\phi_{t,f} = \sum_{\tau=\Delta+L_m-1}^N \mathbf{H}_{\tau,f} s_{t-\tau,f}. \quad (12)$$

The resulting WPE estimate thus contains the target ν , a target estimation error $\tilde{\nu}$, a residue $\tilde{\mathbf{m}}$ from this moderate reverberation and a residue stemming from the final reverberation $\tilde{\phi}$ (again disregarding the error term \mathbf{u} in noiseless scenarios):

$$\begin{aligned} \nu_{t,f}^{(\text{WPE})} &= \mathbf{x}_{t,f} - \mathbf{G}_{t,f}^H \mathbf{X}_{t-\Delta,f} \\ &= \nu_{t,f} + \tilde{\nu}_{t,f} + \tilde{\mathbf{m}}_{t,f} + \tilde{\phi}_{t,f}. \end{aligned} \quad (13)$$

The target estimation error $\tilde{\nu}$ is the target component which was degraded by the algorithm. As described in [30] for the original WPE algorithm, parts of the early reflections may be destroyed because of the inner short-time speech correlations. Under some mild assumptions, the direct path is however fully preserved if the prediction delay Δ is sufficiently large (i.e. larger than the inner speech correlation time). The target estimation error is therefore predicted to be larger when using WPE-based algorithms in the HA scenario—containing more early reflections—than in the CI scenario.

B. Postfiltering scheme

We aim at suppressing the two residues $\tilde{\mathbf{m}}$ and, more particularly, $\tilde{\phi}$. Indeed, $\tilde{\phi}$ is generally of higher magnitude than $\tilde{\mathbf{m}}$, as we will show in the experiments that most of the moderate reverberation is cancelled by efficient WPE-dereverberation.

Additionally, $\tilde{\phi}$ is the more perceptually disturbing of the two residues for the following reasons.

On the one hand, $\tilde{\phi}$ can be considered as speech-like noise which is very poorly correlated to the target signal in comparison to \tilde{m} . On the other hand, as WPE cancels most of the so-called moderate reverberation, there is no preceding energy anymore to mask the late reverberation. The final reverberation residue is then clearly audible.

We thus add a post-filtering enhancement stage after the linear WPE filtering stage, which consists of a single-channel Wiener filter, the phase being left unchanged. This Wiener filter uses estimates of the target PSD $\lambda^{(\nu, \text{PF})}$ and interference PSD $\lambda^{(\tilde{m} + \tilde{\phi}, \text{PF})}$, which can be obtained with classical techniques as decision-directed signal-to-noise ratio (SNR) estimation [32], cepstral smoothing [6], [33], or from a neural network [20], [34].

The resulting estimate is then given for each channel d separately by the celebrated Wiener filter, using the WPE output:

$$\nu_{d,t,f}^{(\text{PF})} = \frac{\lambda_{d,t,f}^{(\nu, \text{PF})}}{\lambda_{d,t,f}^{(\nu, \text{PF})} + \lambda_{d,t,f}^{(\tilde{m} + \tilde{\phi}, \text{PF})}} \nu_{d,t,f}^{(\text{WPE})} \quad (14)$$

C. DNN-based PSD Estimation

We use a DNN-based masking approach to obtain the target and residual reverberation PSDs, similar to what is used to estimate the target speech PSD for WPE filtering (see (6)). At each time step, a frame of the WPE output channel-averaged magnitude $|\bar{\nu}_t^{(\text{WPE})}|$ is fed to a recurrent neural network $\text{MaskNet}_{\text{PF}}$, which outputs both a target and interference mask. An instantaneous periodogram estimate $|\widehat{\eta}|^2$ is then obtained for each channel d through time-frequency masking for each signal $\eta \in \{\nu, \tilde{m} + \tilde{\phi}\}$:

$$|\widehat{\eta}|_{d,t,f}^2 = (\mathcal{M}_{t,f}^{(\eta)} \odot |\nu^{(\text{WPE})}|_{d,t,f})^2. \quad (15)$$

We apply the same channel-averaged mask for all channels using only one instance of the DNN, which saves some computational power and enables us to leave the interaural level differences unchanged. Also, the interaural phase differences are well estimated by WPE linear filtering and are not modified by the post-filtering scheme (see (14)). Therefore the target binaural cues are overall correctly preserved. The corresponding PSD estimate $\lambda^{(\eta, \text{PF})}$ is then obtained through recursive averaging with smoothing factor $\alpha^{(\eta)}$:

$$\lambda_{d,t,f}^{(\eta, \text{PF})} = \alpha^{(\eta)} \lambda_{d,t-1,f}^{(\eta, \text{PF})} + (1 - \alpha^{(\eta)}) |\widehat{\eta}|_{d,t,f}^2. \quad (16)$$

A block diagram of the complete two-stage algorithm is provided in Fig. 1.

D. End-to-End Training Procedure

A baseline approach consists in training the post-filter DNN $\text{MaskNet}_{\text{PF}}$ with a similar mask-based objective:

$$\mathcal{L}_{\text{DNN-PF}} = \sum_{\eta \in \{\nu^{(\text{PF})}, \tilde{m} + \tilde{\phi}\}} \text{KL}(\mathcal{M}_{t,f}^{(\eta)} \odot |\bar{\nu}_{t,f}^{(\text{WPE})}|, |\eta_{t,f}|). \quad (17)$$

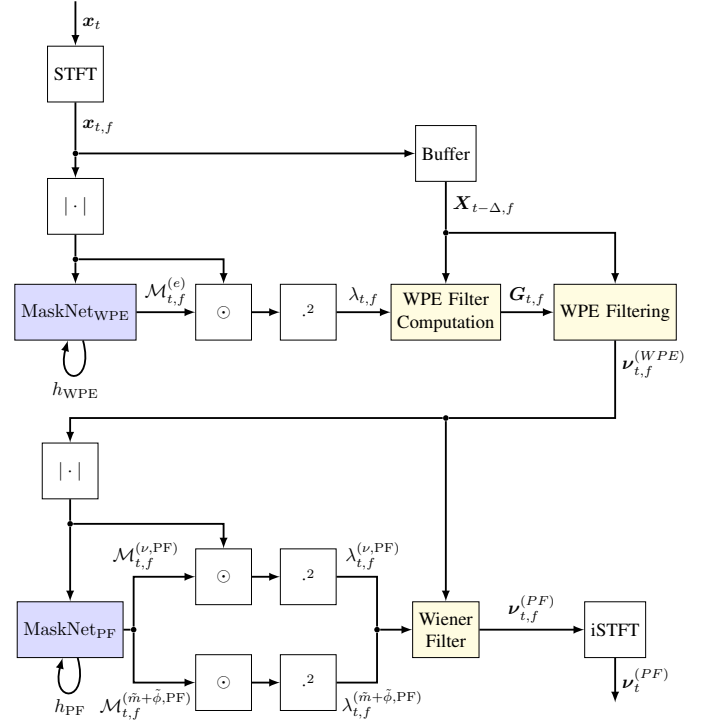


Fig. 1: DNN-supported two-stage dereverberation. Blue blocks refer to trainable neural network layers. Yellow blocks represents adaptive statistical signal processing.

As in Section II, both the DNNs used for WPE filtering and non-linear post-filtering can be fine-tuned with an optimization criterion placed in the time-frequency domain at the final output. The corresponding loss is given as:

$$\mathcal{L}_{\text{E2E-PF}} = \text{KL}(|\nu_{t,f}^{(\text{PF})}|, |\nu_{t,f}|). \quad (18)$$

Algorithm 1 summarizes the complete two-stage end-to-end training procedure. We report results for two approaches. First is **DNN-WPE+DNN-PF**, where the network $\text{MaskNet}_{\text{WPE}}$ is pre-trained with (7), then frozen for the pre-training of $\text{MaskNet}_{\text{PF}}$ with (17). Second is **E2Ep-WPE+DNN-PF**, where the network $\text{MaskNet}_{\text{WPE}}$ is pre-trained with (7) and fine-tuned with (9), then frozen for the pre-training of $\text{MaskNet}_{\text{PF}}$ with (17). We further investigate several training strategies, using the end-to-end objective (18) to fine-tune the post-filter network $\text{MaskNet}_{\text{PF}}$ only, or both networks jointly. These results are not reported in the tables for sake of clarity, but are discussed in Section VI.

A table making the present algorithms correspond to their characteristics and acronyms is given in Table I.

IV. EXPERIMENTAL SETUP

A. Dataset generation

The data generation method resembles that of the WHAMR! dataset [35]. As the initialization time L_i typically corresponds to 4 seconds when using a forgetting factor of $\alpha^{(\text{WPE})} = 0.99$, we concatenate anechoic speech utterances from the WSJ0 dataset belonging to the same speaker, and construct sequences

Algorithm	$\lambda^{(\text{WPE})}$	$\lambda^{(\nu, \text{PF})}, \lambda^{(\tilde{m} + \tilde{\phi}, \text{PF})}$
RLS-WPE [19]	Reverberant	\times
O-PSD-WPE	Oracle	\times
DNN-PF	\times	$\mathcal{L}_{\text{DNN-PF}}$
DNN-WPE	$\mathcal{L}_{\text{DNN-WPE}}$	\times
E2Ep-WPE	$\mathcal{L}_{\text{DNN-WPE}} \rightarrow \mathcal{L}_{\text{E2E-WPE}}$	\times
DNN-WPE+DNN-PF	$\mathcal{L}_{\text{DNN-WPE}}$	$\mathcal{L}_{\text{DNN-PF}}$
E2Ep-WPE+DNN-PF	$\mathcal{L}_{\text{DNN-WPE}} \rightarrow \mathcal{L}_{\text{E2E-WPE}}$	$\mathcal{L}_{\text{DNN-PF}}$

TABLE I: Correspondance between used acronyms and training strategies for estimating the PSDs used in the linear filtering and non-linear post-filtering stages.

Algorithm 1 Two-Stage End-to-End Training Procedure

- 1: Extract STFT of given sequence
 - 2: Segment sequence in N segments of size L
 - 3: **for** $n \in \{0 \dots N - 1\}$ **do**
 - 4: **if** $n = 0$ **then** \triangleright Initialization period
 - 5: Initialize DNN hidden states $h_0^{(n)} = \mathbf{0}$
 - 6: Initialize WPE and post-filter statistics
 - $\mathbf{G}_{0,f}^{(0)} = \mathbf{0}, (\mathbf{R}^{-1})_{0,f}^{(0)} = \mathbf{I}$
 - $\lambda_{0,f}^{(\nu, \text{PF}, 0)} = \mathbf{0}, \lambda_{0,f}^{(\tilde{m} + \tilde{\phi}, \text{PF}, 0)} = \mathbf{0}$
 - 7: **for** $t \in \{0 \dots L - 1\}$ **do**
 - 8: Compute $\nu_{t,f}^{(\text{PF})}$
 - 9: **if** $n > 0$ **then** \triangleright After initialization
 - 10: Initialize DNN hidden states $h_0^{(n)} = h_{L-1}^{(n-1)}$
 - 11: Initialize WPE and post-filter statistics
 - $\mathbf{G}_{0,f}^{(n)} = \mathbf{G}_{L-1,f}^{(n-1)}, (\mathbf{R}^{-1})_{0,f}^{(n)} = (\mathbf{R}^{-1})_{L-1,f}^{(n-1)}$
 - $\lambda_{0,f}^{(\nu, \text{PF}, n)} = \lambda_{L-1,f}^{(\nu, \text{PF}, n-1)}, \lambda_{0,f}^{(\tilde{m} + \tilde{\phi}, \text{PF}, n)} = \lambda_{L-1,f}^{(\tilde{m} + \tilde{\phi}, \text{PF}, n-1)}$
 - 12: **for** $t \in \{0 \dots L - 1\}$ **do**
 - 13: Compute $\nu_{t,f}^{(\text{PF})}$
 - 14: Backpropagate loss (18) through time on n
 - 15: Repeat [12:] to update statistics and states
-

of approximately 20 seconds. Within each sequence, permutations of the utterances are used to create several versions of the sequence, since the first segment is never explicitly used for optimization (cf Algorithm 1).

These sequences are convolved with 2-channel RIRs generated with the RAZR engine [36] and randomly picked. Each RIR is generated by uniformly sampling room acoustics parameters as in [35] and a T_{60} reverberation time between 0.4 and 1.0 seconds. Head-Related Transfer Function based auralization is performed in the RAZR engine, using a KEMAR dummy head response from the MMHR-HRTF database [37].

As target data for the HA case, the first 40 ms of the RIR is convolved with the utterance, representing the direct path and the early reflections.

For the CI scenario, only the first 16 ms of the RIR are

used, as estimating the direct path only from reverberant speech provided poor results for instrumental measures and informal listening, both when looking at the output of the MaskNet_{WPE} and the complete WPE stage. As the goal is to obtain optimal WPE results, the target should match the best possible linear prediction estimate one can get, which is limited by the prediction delay protecting the inner speech correlations (~ 10 ms). Therefore, the minimal prediction delay given the STFT frame length should be set to $\Delta = 2$ frames, that is, 16 ms with the hyperparameters described below. We further noticed that with this setting, very few early reflections could be heard in the target, and no direct path speech distortion could be heard or instrumentally predicted in the linear prediction estimate when using oracle target PSD.

Ultimately, each training set consists of approximately 55 hours of speech data sampled at 16 kHz.

B. Hyperparameter settings

All approaches are trained using the Adam optimizer with a learning rate of 10^{-4} , exponentially decreasing by 0.96 at every epoch. Early stopping with a patience of 20 epochs and mini-batches size of 128 segments are used. The STFT uses a square-rooted Hann window of 32 ms and a 75 % overlap, and segments of $L_i = 4$ s are constructed from each sequence.

The WPE filter length is set to $K = 10$ STFT frames (i.e. 80 ms), the number of channels to $D = 2$, the WPE adaptation factor to $\alpha^{(\text{WPE})} = 0.99$ and the delays to $\Delta_{\text{HA}} = 5$ frames (i.e. 40 ms) for the HA scenario and $\Delta_{\text{CI}} = 2$ (i.e. 16 ms) frames for the CI scenario. Those delay values are picked as they correspond to the amount of early reflections contained in the respective target, and they experimentally provide optimal evaluation metrics when comparing the corresponding target to the output of WPE when using the oracle PSD.

We use the Wiener Filter as post-filter estimator, as the corresponding operations are the most straightforward to use for backpropagation with the end-to-end training procedure Algorithm 1. A MMSE Log Spectral Amplitude estimator [32] or a super-Gaussian MMSE estimator [33] provide slightly better results, but finding a form fit for efficient backpropagation is not straightforward so we stick to the Wiener filter for sake of simplicity and ease of comparison between strategies. Adaptation factors are set to $\alpha^{(\nu)} = \alpha^{(\tilde{m} + \tilde{\phi})} = 0.40$ for the target and residual reverberation.

The DNN used in [20] is composed of a single long-short term memory (LSTM) layer with 512 units followed by two

linear layers with rectified linear activations (ReLU), and a linear output layer with sigmoid activation. We remove the two ReLU-activated layers in our experiments, which did not degrade the dereverberation performance, while reducing the number of trainable parameters by 75 %. We use the same architecture for MaskNet_{WPE} and MaskNet_{PF}.

We estimate the number of MAC operations per second of the two-stage algorithm to 28.7 GMAC·s⁻¹ at 16 kHz. This setting allows to obtain a real-time factor—defined as the ratio between the time needed to process an utterance and the length of the utterance—below 0.1 with all computations performed on a Nvidia GeForce RTX 2080Ti GPU.

C. Evaluation metrics

We evaluate all approaches on the described test sets corresponding to the HA and CI scenarios.

Following the definition of the early-to-late reverberation ratio (ELR) [10], [38], we introduce two new instrumental measures: the *early-to-mid reverberation ratio* (EMR) and *early-to-final reverberation ratio* (EFR). Coefficients $\{\hat{H}\}_{d,\tau,f}$ of order $0 \leq \tau \leq P-1$ are computed for each channel d and frequency bin f separately, in order to minimize a minimum mean square error regression objective in the time-frequency domain between Y and the dry utterance S filtered by H :

$$\{\hat{H}_{d,\tau,f}\}_{\tau} = \arg \min_H \|Y_{d,t,f} - \sum_{\tau=0}^{P-1} H_{d,\tau,f} S_{t-\tau-\delta^*,f}\|_2^2, \quad (19)$$

with δ^* being the oracle propagation delay obtained by looking for the direct path in the true RIR. This delay is used so as not to try and estimate RIR coefficients preceding the propagation delay which are supposed to be zero, therefore reducing the estimation error. The estimation error is further reduced by choosing the order P to match the T_{30} of the true RIR rather than the T_{60} , as the estimation noise floor was found to be close to -30 dB.

The channel-wise RIRs are then stacked and the target, moderate and final reverberation components are estimated as:

$$\hat{\mathbf{v}}_{t,f} = \sum_{\tau=0}^{\tilde{\Delta}-1} \hat{H}_{\tau,f} S_{t-\tau-\delta^*,f}, \quad (20)$$

$$\hat{\mathbf{m}}_{t,f} = \sum_{\tau=\tilde{\Delta}}^{\tilde{\Delta}+L_m-1} \hat{H}_{\tau,f} S_{t-\tau-\delta^*,f}, \quad (21)$$

$$\hat{\boldsymbol{\phi}}_{t,f} = \sum_{\tau=\tilde{\Delta}+L_m}^{P-1} \hat{H}_{\tau,f} S_{t-\tau-\delta^*,f}. \quad (22)$$

We set $\tilde{\Delta} = 5$ (i.e. 40ms) in the hearing-aided case and $\tilde{\Delta} = 2$ (i.e. 16ms) in the cochlear-implanted scenario as explained in the target specifications. We set the moderate range length to $L_m = K = 10$ (i.e. 80ms).

The ELR, EMR and EFR are then defined as:

$$\text{ELR} = 10 \log_{10} \left(\|\hat{\mathbf{v}}_{t,f}\|^2 / \|\hat{\mathbf{m}}_{t,f} + \hat{\boldsymbol{\phi}}_{t,f}\|^2 \right), \quad (23)$$

$$\text{EMR} = 10 \log_{10} \left(\|\hat{\mathbf{v}}_{t,f}\|^2 / \|\hat{\mathbf{m}}_{t,f}\|^2 \right), \quad (24)$$

$$\text{EFR} = 10 \log_{10} \left(\|\hat{\mathbf{v}}_{t,f}\|^2 / \|\hat{\boldsymbol{\phi}}_{t,f}\|^2 \right). \quad (25)$$

We complete the evaluation benchmark with the Perceptual Objective Listening Quality Analysis (POLQA)¹, the signal-to-distortion ratio (SDR) and signal-to-noise ratio [39].

V. EXPERIMENTAL RESULTS AND DISCUSSION

A. Compared algorithms

We apply the different strategies mentioned in sections II and III and compare their results in figures 2 and 3 for the HA and CI scenarios respectively. Spectrograms are also plotted in Fig. 4. We add to the various proposed end-to-end approaches the RLS-WPE with oracle PSD (**O-PSD-WPE**, [19]) and the RLS-WPE with PSD estimated by a DNN on a frame-to-frame basis (**DNN-WPE**, [20]). We also report the performance of the approach denoted as **DNN-PF**, where the output of the network MaskNet_{WPE} is directly used for Wiener non-linear filtering, eluding the WPE linear filter step.

VI. DISCUSSION

A. Moderate Reverberation Suppression

We first validate the method used for deriving the ELR, EMR and EFR metrics, described in IV-C. We plot the log-energies of the true RIR, the RIR estimated with (19) and the transfer function of the concatenation of the room with the O-PSD-WPE algorithm on Fig. 5. We observe that in the chosen T_{30} range, the true and estimated RIRs match almost perfectly, showing the validity of this MMSE-based estimation for linear transfer function estimation in this range. We also observe a strong dereverberation performance of the O-PSD-WPE algorithm in the filter range as well as shortly after this range, which is the effect of recursive averaging. However, we note that because of the adaptive nature of the algorithm and the nonlinear LSTM dynamics, the observed transfer function is only the result of a linearization of the true system. This limits the use of a graphical comparison of algorithms and we rather use the derived ELR, EMR and EFR metrics, which correlate well with informal listening experiments.

The ELR metric in figures 2 and 3 indicate a superior dereverberation performance of E2Ep-WPE in comparison to DNN-WPE, i.e. when the DNN MaskNet_{WPE} is fine-tuned end-to-end. The high EMR difference indicates that the moderate reverberation in the range $[\tilde{\Delta}, \tilde{\Delta} + L_m - 1]$ is particularly well suppressed. As already mentioned in [25], this stems from the better dereverberation performance in the range which is available to the WPE linear filter, through end-to-end optimization of the neural network MaskNet_{WPE}.

B. Residual Reverberation Suppression

As displayed in figures 2 and 3, using a DNN-assisted enhancement scheme highly improves the dereverberation performance on the basis of WPE linear filtering, and yields much superior POLQA score. The high EFR improvement indicates that post-filtering mostly focuses on removing the final reverberation, i.e. after the range accessible to WPE filtering. In particular, the E2Ep-WPE+DNN-PF approach

¹Wideband MOS score, following standard ITU-T P.863. The authors would like to thank Rohde & Schwarz SwissQual AG for their support with POLQA.

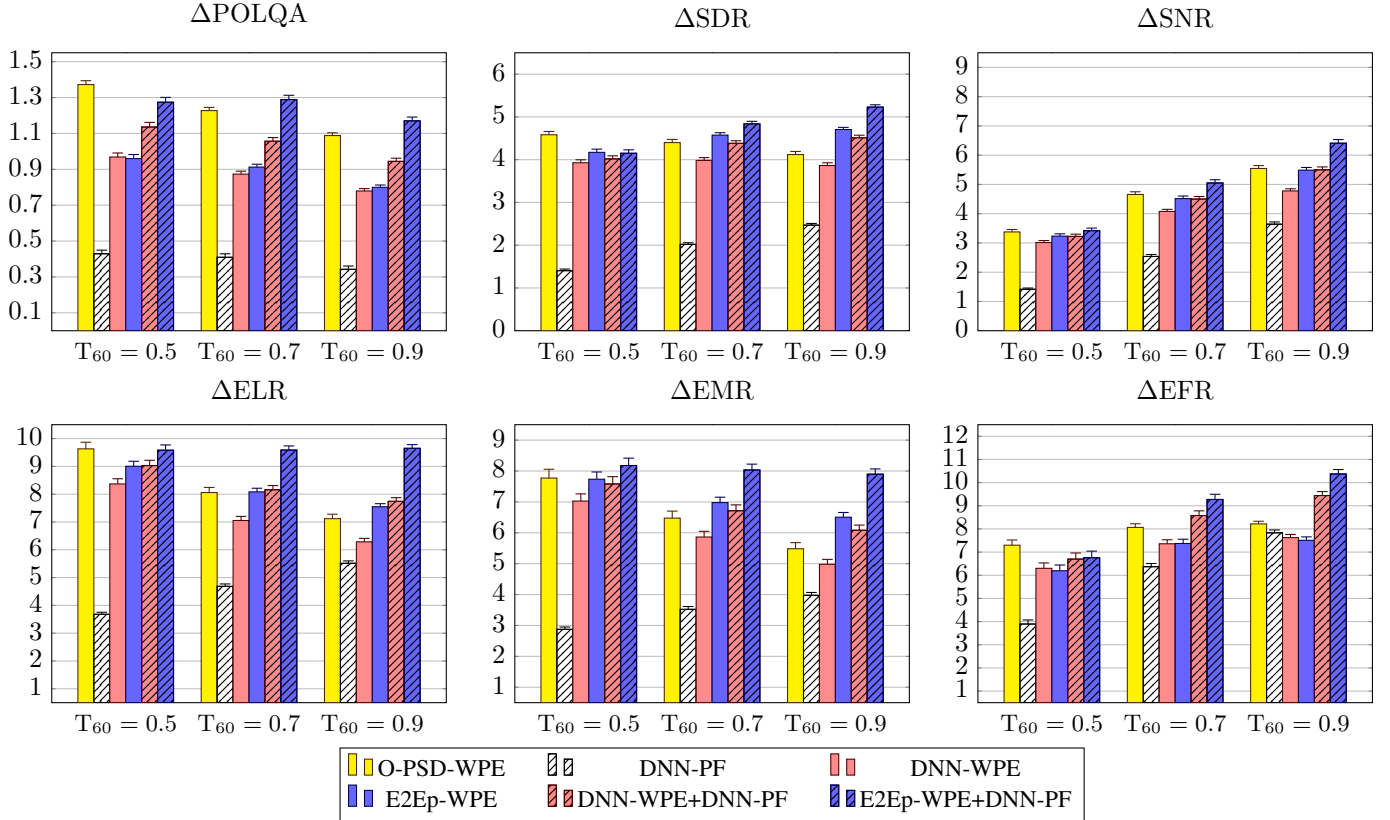


Fig. 2: Improvements upon unprocessed reverberant signals for hearing-aided scenario. All metrics except POLQA are in dB. T_{60} times indicated in s. [$\nu = d + e$; $\Delta = \hat{\Delta} = 5$]

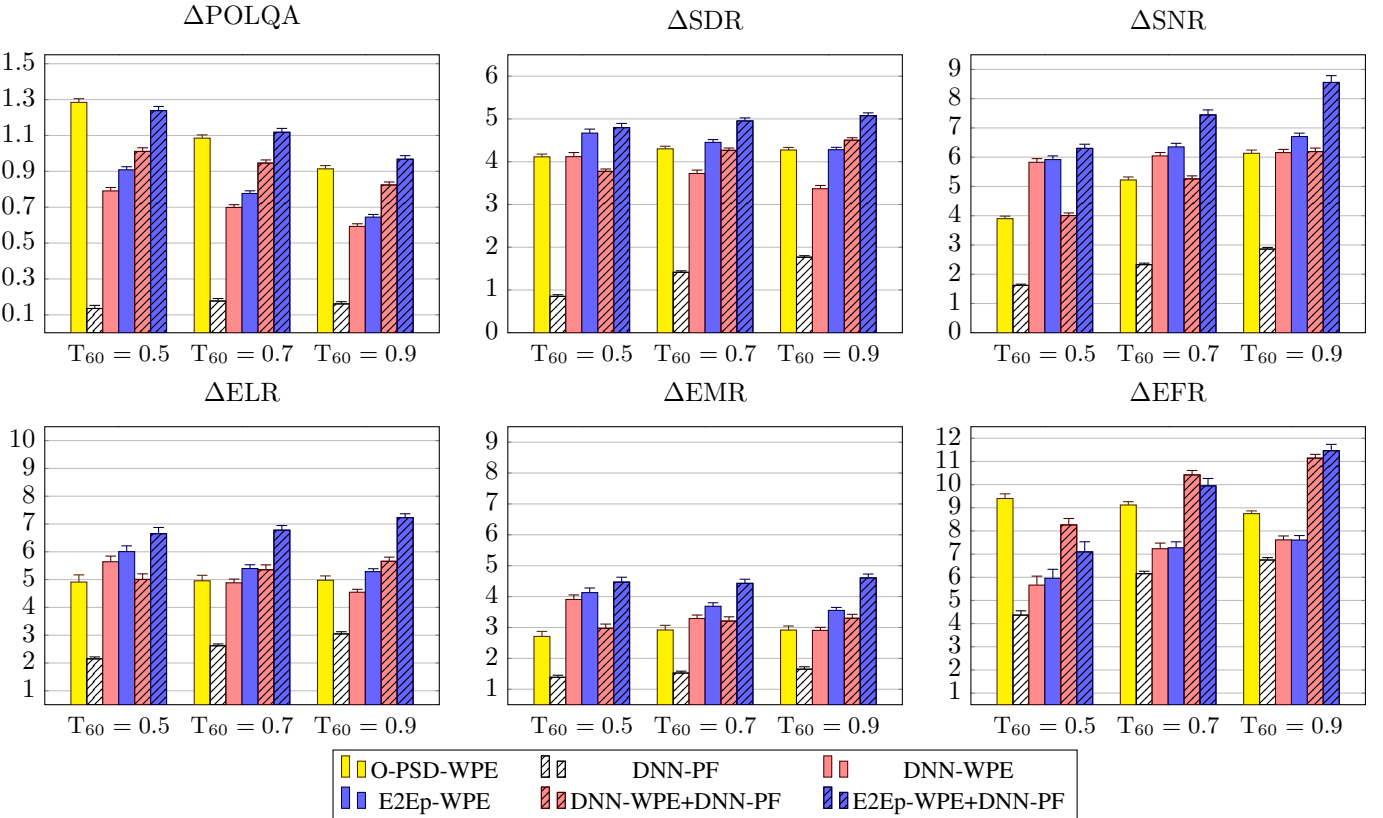


Fig. 3: Improvements upon unprocessed reverberant signals results for cochlear-implanted scenario. All metrics except POLQA are in dB. T_{60} times indicated in s. [$\nu = d$; $\Delta = \hat{\Delta} = 2$]

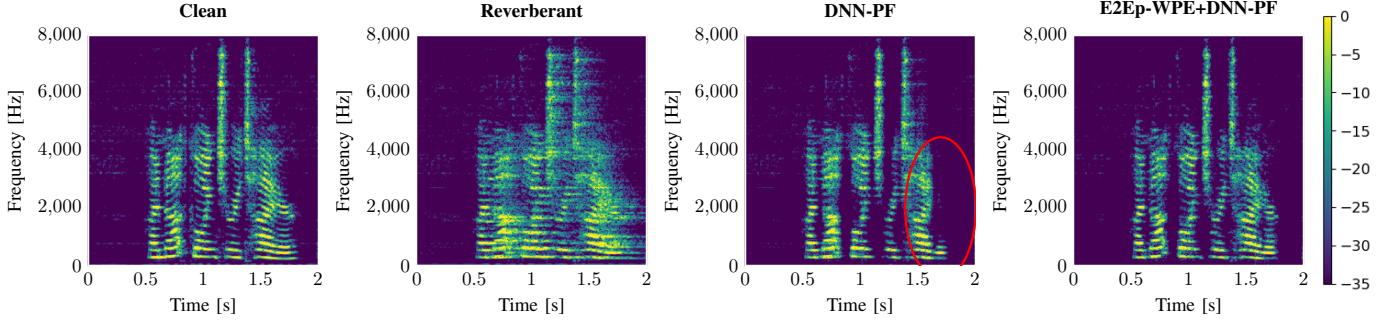


Fig. 4: Log-energy spectrograms of clean, reverberant and processed utterances. $T_{60} = 0.68s$. HA scenario [$\nu = d + e$; $\Delta = \tilde{\Delta} = 5$] Heavy speech distortions can be observed in the DNN-PF output, as highlighted in the red ellipse.

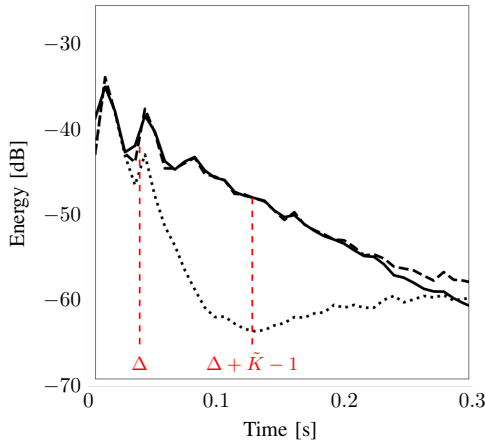


Fig. 5: Comparison of the true RIR (full line) vs. the Estimated RIR (dashed line). Estimated linearized transfer function of the system which applies O-PSD-WPE on reverberant speech is shown as a dotted line. We observe strong dereverberation in the given filter range $[\Delta, \Delta + \tilde{K} - 1]$, and shortly afterwards because of recursive averaging. Only the T_{30} range is displayed as it is the valid estimation range for the estimated RIR. $T_{60} = 0.8s$. HA scenario [$\nu = d + e$; $\Delta = \tilde{\Delta} = 5$]

which uses a pretrained network for post-filtering on top of end-to-end trained WPE filtering, outperforms all other approaches on all metrics. In comparison, using only the post-filter without WPE filtering introduces a lot of speech distortion, as shown in Fig. 4. Similarly, the DNN-WPE+DNN-PF performance indicates that using the post-filtering stage on the output of the DNN-WPE algorithm—without fine-tuning $\text{MaskNet}_{\text{WPE}}$ with our end-to-end procedure—yields poorer results (final POLQA is 0.2 lower and SNR is 1dB lower than E2Ep-WPE+DNN-PF). This shows that removing the moderate reverberation with WPE linear filtering is an essential step before using a speech enhancement scheme like our post-filter. Since E2Ep-WPE efficiently removes the moderate reverberation, as measured by EMR, it provides a particularly good ground for enhancement-like post-filtering, since only the reverberation tail remains, and provides the best EFR and POLQA performance.

C. Reverberation Times

For a given scenario, the dereverberation task becomes increasingly difficult as the T_{60} time grows longer. We observe for example that using the oracle PSD for WPE performs well only for low T_{60} reverberation times because of the limited filter length, and the performance gap between this approach and the proposed two-stage approach increases with the T_{60} reverberation time.

Furthermore, we notice an increasing gap in SNR and EFR between DNN-WPE+DNN-PF and E2Ep-WPE+DNN-PF as the T_{60} grows larger, which seems to indicate that our best performing approach E2Ep-WPE+DNN-PF is more robust to challenging reverberation conditions.

D. End-to-End Training Strategies

The best performing approach on all metrics is E2Ep-WPE+DNN-PF—with very few exceptions across T_{60} reverberation times. Further fine-tuning the post-filter network $\text{MaskNet}_{\text{PF}}$ did not provide better results nor did fine-tuning the two networks simultaneously. Directly training the two networks with the end-to-end training criterion (18) significantly worsened the performance, showing the importance of our pre-training strategy.

E. Hearing Device Users Categories Specialization

Similar trends in performances are observed for the hearing-aided and cochlear-implanted scenarios, with two noticeable differences.

First, dereverberation is a more complicated task in the cochlear-implanted scenario as compared to the hearing-aided scenario, as the input ELR and SDR scores are lower. However, the POLQA, SDR and SNR score improvements stay relatively consistent across both scenarios, highlighting the robustness of our approach. On the other hand, the ELR, EMR and EFR score improvements vary across scenarios, with higher ELR and EMR improvements for the hearing-aided scenario and higher EFR improvements for the cochlear-implanted scenario.

We take a deeper look at the cochlear-implanted scenario to explain the mentioned gaps between hearing-aided and cochlear-implanted scenarios. We emphasize that the design

choice $\Delta_{CI} = \tilde{\Delta}_{CI} = 2$ is instrumental in matching the capacity of ideal WPE filtering with the target for training and evaluation, as the prediction delay needs to be superior to the inner-speech correlations. However, this causes two problems. The first issue is that there is a mismatch between our designed target and the true target i.e. the direct path only, but we argue that this mismatch is hardly noticeable in listening experiments. The second is the poorer ELR, EMR and SDR performance of O-PSD-WPE which indicates that the target signal was distorted, which we explain as follows. As mentioned in III-A, the initial role of the prediction delay Δ is to prevent the destruction of short-term speech correlations. A side effect is that Δ also protects some of the early reflections. However, given the recursive nature of RLS-WPE, information about the early reflections leaks to the estimation of the late reverberation (see (5)), thus partially destroying these early reflections. Therefore, using a particularly short Δ can cause some of the early reflections contained in the target to be destroyed, resulting in the observed distortions.

This destruction of the early reflections is also true for the hearing-aided scenario, but the effect is less dramatic as the destroyed early reflections represent a lesser fraction of the target signal, compared to that of the cochlear-implanted scenario. This explains the different ELR and EMR score improvements across scenarios. Finally, we argue that, for our parameters choice, the inner speech correlations are well preserved, as the POLQA score remains very high in both scenarios, which is confirmed by listening experiments.

F. Extension to noisy scenarios

As stated in Section II, noisy scenarios are not explicitly taken into account throughout this study. The regularization parameter ϵ added in (3) simply increases the robustness of WPE to modelling errors and noise. Our study could be combined with approaches tackling joint dereverberation and denoising such as [40] where WPE for dereverberation is unified with a MVDR beamformer for denoising, both in an online fashion. Joint dereverberation and denoising is also tackled combining sparsity promotion with a denoising penalty as presented in [41] (chapter 7).

VII. CONCLUSION

We proposed a two-stage DNN-assisted algorithm for adaptive frame-online multi-channel dereverberation in a noiseless scenario. The first stage consists of multi-frame, multi-channel linear filtering with help of a DNN estimating the target speech PSD. This first stage was shown to focus on accurately removing moderate reverberation up to the given filter range, in our case, 120 ms. The second stage performs channel-wise, single-frame non-linear spectral enhancement with help of a DNN estimating the target and interference PSDs. This second stage was able to efficiently remove residual reverberation left off by the first stage, as the residue was perceptually close to noise.

Instrumental metrics like the early-to-late reverberation ratio and its variants confirmed the listening-based experiments showing the complementary aspect of the two proposed stages.

REFERENCES

- [1] P. Naylor and N. Gaubitch, *Speech Dereverberation*, vol. 59. 01 2011.
- [2] E. Habets, *Single- and Multi-Microphone Speech Dereverberation Using Spectral Enhancement*. PhD thesis, 01 2007.
- [3] A. Kuklasinski, S. Doclo, T. Gerkmann, S. Holdt Jensen, and J. Jensen, "Multi-channel PSD estimators for speech dereverberation - a theoretical and experimental comparison," in *IEEE Int. Conf. Acoustics, Speech, Signal Proc. (ICASSP)*, pp. 91–95, 2015.
- [4] B. Cauchi, I. Kodrasi, R. Rehr, S. Gerlach, A. Jukic, T. Gerkmann, S. Doclo, and S. Goetze, "Combination of MVDR beamforming and single-channel spectral processing for enhancing noisy and reverberant speech," *EURASIP Journal on Advances in Signal Proc.*, vol. 2015, pp. 1–12, 2015.
- [5] A. Schwarz and W. Kellermann, "Coherent-to-diffuse power ratio estimation for dereverberation," *IEEE/ACM Trans. Audio, Speech, Language Proc.*, vol. 23, no. 6, pp. 1006–1018, 2015.
- [6] T. Gerkmann, "Cepstral weighting for speech dereverberation without musical noise," in *2011 19th European Signal Processing Conference*, pp. 2309–2313, 2011.
- [7] T. Nakatani, T. Yoshioka, K. Kinoshita, M. Miyoshi, and B. Juang, "Blind speech dereverberation with multi-channel linear prediction based on short time fourier transform representation," in *ICASSP 2008*, pp. 85–88, 2008.
- [8] A. Jukić, T. van Waterschoot, T. Gerkmann, and S. Doclo, "Multi-channel linear prediction-based speech dereverberation with sparse priors," *IEEE/ACM Trans. Audio, Speech, Language Proc.*, vol. 23, no. 9, pp. 1509–1520, 2015.
- [9] J. S. Bradley, H. Sato, and M. Picard, "On the importance of early reflections for speech in rooms," *The Journal of the Acoustical Society of America*, vol. 113, no. 6, pp. 2947–2952, 2003.
- [10] T. Yoshioka, T. Nakatani, M. Miyoshi, and H. G. Okuno, "Blind separation and dereverberation of speech mixtures by joint optimization," *IEEE Trans. Audio, Speech, Language Proc.*, vol. 19, no. 1, pp. 69–84, 2011.
- [11] H. Kagami, H. Kameoka, and M. Yukawa, "Joint separation and dereverberation of reverberant mixtures with determined multichannel non-negative matrix factorization," in *IEEE Int. Conf. Acoustics, Speech, Signal Proc. (ICASSP)*, pp. 31–35, 2018.
- [12] K. Kinoshita, M. Delcroix, H. Kwon, T. Mori, and T. Nakatani, "Neural network-based spectrum estimation for online WPE dereverberation," in *ISCA Interspeech*, 2017.
- [13] Z.-Q. Wang, G. Wichern, and J. L. Roux, "Convolutional prediction for monaural speech dereverberation and noisy-reverberant speaker separation," 2021.
- [14] K. Han, Y. Wang, D. Wang, W. S. Woods, I. Merks, and T. Zhang, "Learning spectral mapping for speech dereverberation and denoising," *IEEE/ACM Trans. Audio, Speech, Language Proc.*, vol. 23, no. 6, pp. 982–992, 2015.
- [15] D. S. Williamson and D. Wang, "Time-frequency masking in the complex domain for speech dereverberation and denoising," *IEEE/ACM Trans. Audio, Speech, Language Proc.*, vol. 25, no. 7, pp. 1492–1501, 2017.
- [16] Y. Luo and N. Mesgarani, "Real-time single-channel dereverberation and separation with time-domain audio separation network," 2018.
- [17] B. Schwartz, S. Gannot, and E. A. P. Habets, "Online speech dereverberation using Kalman filter and EM algorithm," *IEEE/ACM Trans. Audio, Speech, Language Proc.*, vol. 23, no. 2, pp. 394–406, 2015.
- [18] S. Braun and E. A. P. Habets, "Online dereverberation for dynamic scenarios using a Kalman filter with an autoregressive model," *IEEE Signal Proc. Letters*, vol. 23, no. 12, pp. 1741–1745, 2016.
- [19] T. Yoshioka, H. Tachibana, T. Nakatani, and M. Miyoshi, "Adaptive dereverberation of speech signals with speaker-position change detection," in *IEEE Int. Conf. Acoustics, Speech, Signal Proc. (ICASSP)*, pp. 3733–3736, 2009.
- [20] J. Heymann, L. Drude, R. Haeb-Umbach, K. Kinoshita, and T. Nakatani, "Frame-online DNN-WPE dereverberation," *IWAENC*, pp. 466–470, 2018.
- [21] X. Chang, W. Zhang, Y. Qian, J. L. Roux, and S. Watanabe, "Mimo-speech: End-to-end multi-channel multi-speaker speech recognition," *2019 IEEE Automatic Speech Recognition and Understanding Workshop (ASRU)*, pp. 237–244, 2019.
- [22] T. Ochiai, S. Watanabe, T. Hori, J. R. Hershey, and X. Xiao, "Unified architecture for multichannel end-to-end speech recognition with neural beamforming," *IEEE Journal of Selected Topics in Signal Proc.*, vol. 11, no. 8, pp. 1274–1288, 2017.

- [23] W. Zhang, C. Boeddeker, S. Watanabe, T. Nakatani, M. Delcroix, K. Kinoshita, T. Ochiai, N. Kamo, R. Haeb-Umbach, and Y. Qian, "End-to-end dereverberation, beamforming, and speech recognition with improved numerical stability and advanced frontend," in *IEEE Int. Conf. Acoustics, Speech, Signal Proc. (ICASSP)*, 2021.
- [24] J. Heymann, L. Drude, R. Haeb-Umbach, K. Kinoshita, and T. Nakatani, "Joint optimization of neural network-based WPE dereverberation and acoustic model for robust online ASR," in *IEEE Int. Conf. Acoustics, Speech, Signal Proc. (ICASSP)*, 2019.
- [25] J.-M. Lemercier, J. Thiemann, R. König, and T. Gerkmann, "Customizable end-to-end optimization of neural network-supported dereverberation for hearing devices," in *IEEE Int. Conf. Acoustics, Speech, Signal Proc. (ICASSP)*, 2022.
- [26] Y. Hu and K. Kokkinakis, "Effects of early and late reflections on intelligibility of reverberated speech by cochlear implant listeners," *The Journal of the Acoustical Society of America*, vol. 135, pp. EL22–8, 01 2014.
- [27] Z.-Q. Wang and D. Wang, "Deep learning based target cancellation for speech dereverberation," *IEEE/ACM Trans. Audio, Speech, Language Proc.*, vol. 28, pp. 941–950, 2020.
- [28] L. Drude, C. Bøddeker, J. Heymann, R. Haeb-Umbach, K. Kinoshita, M. Delcroix, and T. Nakatani, "Integrating neural network based beamforming and weighted prediction error dereverberation," in *INTER-SPEECH*, 2018.
- [29] I. Cohen, "Optimal speech enhancement under signal presence uncertainty using log-spectral amplitude estimator," *IEEE Signal Processing Letters*, vol. 9, no. 4, pp. 113–116, 2002.
- [30] T. Nakatani, T. Yoshioka, K. Kinoshita, M. Miyoshi, and B.-H. Juang, "Speech dereverberation based on variance-normalized delayed linear prediction," *IEEE Trans. Audio, Speech, Language Proc.*, vol. 18, no. 7, pp. 1717–1731, 2010.
- [31] A. Cichocki and S.-i. Amari, "Families of alpha- beta- and gamma-divergences: Flexible and robust measures of similarities," *Entropy*, vol. 12, no. 6, pp. 1532–1568, 2010.
- [32] Y. Ephraim and D. Malah, "Speech enhancement using a minimum mean-square error log-spectral amplitude estimator," *IEEE Trans. Audio, Speech, Language Proc.*, vol. 33, no. 2, pp. 443–445, 1985.
- [33] C. Breithaupt, M. Krawczyk, and R. Martin, "Parameterized mmse spectral magnitude estimation for the enhancement of noisy speech," in *IEEE Int. Conf. Acoustics, Speech, Signal Proc. (ICASSP)*, pp. 4037–4040, 2008.
- [34] O. Ernst, S. E. Chazan, S. Gannot, and J. Goldberger, "Speech dereverberation using fully convolutional networks," 2019.
- [35] M. Maciejewski, G. Wichern, E. McQuinn, and J. L. Roux, "Whamr!: Noisy and reverberant single-channel speech separation," 2020.
- [36] T. Wendt, S. Van De Par, and S. D. Ewert, "A computationally-efficient and perceptually-plausible algorithm for binaural room impulse response simulation," *Journal of the Audio Engineering Society*, vol. 62, pp. 748–766, november 2014.
- [37] J. Thiemann and S. van de Pars, "A multiple model high-resolution head-related impulse response database for aided and unaided ears," *EURASIP Journal on Advances in Signal Processing*, 2019.
- [38] G. Carbajal, R. Serizel, E. Vincent, and E. Humbert, "Joint NN-supported multichannel reduction of acoustic echo, reverberation and noise," *IEEE/ACM Trans. Audio, Speech, Language Proc.*, vol. 28, pp. 2158–2173, 2020.
- [39] E. Vincent, R. Gribonval, and C. Fevotte, "Performance measurement in blind audio source separation," *IEEE/ACM Trans. Audio, Speech, Language Proc.*, vol. 14, no. 4, pp. 1462–1469, 2006.
- [40] T. Nakatani and K. Kinoshita, "Simultaneous denoising and dereverberation for low-latency applications using frame-by-frame online unified convolutional beamformer," in *ISCA Interspeech*, 2019.
- [41] A. Jukic, *Sparse Multi-Channel Linear Prediction for Blind Speech Dereverberation*. PhD thesis, 2017.